Soft Matter

PAPER

View Article Online
View Journal | View Issue



Cite this: *Soft Matter*, 2019, **15**, 3027

# *In vivo* adhesion force measurements of *Chlamydomonas* on model substrates

Christian Titus Kreis,† Alice Grangier and Oliver Bäumchen *

The initial stages of biofilm formation at a surface are triggered by the surface association of individual microorganisms. The biological mechanisms and interfacial interactions underlying microbial adhesion to surfaces have been widely studied for bacteria, while microalgae remained rather unconsidered despite their technological relevance, *e.g.*, in photo-bioreactors. We performed *in vivo* micropipette force measurements with the model organism *Chlamydomonas reinhardtii*, a unicellular eukaryotic microalga that dwells in liquid-infused soils and on moist rocks. We characterize the adhesion forces and dissect the influence of intermolecular interactions by probing the adhesion forces of single cells on different model substrates with tailored properties. Our experiments show that the flagella-mediated adhesion of *Chlamydomonas* to surfaces is largely substrate independent, enabling the cell to adhere to any type of surface. This universal adhesion mechanism allows the microalga to effectively colonize abiotic surfaces in their heterogeneous natural habitats. Our results reveal a dominant contribution of electrostatic interactions governing microalgal adhesion and suggest that flagella membrane processes may cause significant variations of the adhesive properties of the flagella.

Received 1st November 2018,
Accepted 5th March 2019

DOI: 10.1039/c8sm02236d

rsc.li/soft-matter-journal



Microorganisms can be found on many biotic and abiotic surfaces. Their natural habitats are rather diverse and the surfaces that microbes colonize are typically heterogeneous in their topography as well as in their chemical composition. The chemical compositions of the surface and the underlying substrate determine the interfacial interactions that cells experience in close proximity to a substrate. Indeed, understanding the intermolecular interactions that govern microbial surface colonization is imperative to develop physicochemical pathways for dealing with biofilm-related issues in natural and technological settings.

Microbial adhesion strategies have been extensively studied for bacteria due to their outstanding relevance in biomedical applications.[1] Bacterial adhesion is generally mediated by membrane proteins and cellular appendages, like pili and fimbrae, that are often tailored to attach to extracellular material in a host or biofilm, but also enable adhesion to abiotic surfaces.[2–6] Atomic force microscopy techniques have been widely employed to study the intermolecular interactions that mediate the adhesion of living bacteria to different substrates.[7–9] In contrast to bacteria as well as other representatives of microbial life, *e.g.* slime molds,[10,11] microalgae remained rather unconsidered so far.

Microalgae are photoactive, eukaryotic microorganisms that form the phytoplankton of salt and freshwater ecosystems, which contribute to the global nutrient cycles and represent the basis of food chains.[12–15] Although they often live freely suspended in open water bodies, microalgae also colonize light-exposed surfaces in moist habitats, like soil, temporary pools, and streams. On surfaces, microalgae may form biofilms (often in symbiosis with bacteria), which represent a major contribution to biofouling in the aqueous environments of various industrial scenarios, like water cooling systems and ship hulls.[16,17] Despite the fact that microalgae inherit profound ecological and technological importance, *e.g.* for the production of biofuels and drug components in photo-bioreactors, quantitative single-cell adhesion measurements are lacking and microalgal adhesion strategies remain elusive so far. Adhesion studies are limited to force measurements on the adhesive glycoproteins and nanofibres secreted by green algae and diatoms, respectively.[18,19]

The unicellular, bi-flagellated microalga *Chlamydomonas reinhardtii* is a model organism to study cellular processes, *e.g.* flagella biology, cilia-related diseases, and microbial motility.[20,21] *Chlamydomonas* shares many common features of flagellated microalgae, *e.g.* the circadian life cycle, sexual and asexual reproduction, and the fact that it can be found in a free-swimming (planktonic) as well as a surface-associated state. Its surface association is enabled by flagella-surface contacts, which are mediated by adhesive interactions between the flagella membrane glycoprotein (FMG-1B) and the surface.[22] Furthermore, the adhesive contact enables the cell to move on the surface, called gliding

*Max Planck Institute for Dynamics and Self-Organization (MPIDS), Am Faßberg 17, D-37077 Göttingen, Germany. E-mail: oliver.baeumchen@ds.mpg.de*

† Present address: Department of Physical and Environmental Sciences, University of Toronto-Scarborough, 1065 Military Trail, Toronto, Ontario, Canada.

motility,[23] which is widely studied as a model for the dynamics of molecular motors and cellular force transduction.[24,25]

*Chlamydomonas* is equipped with a variety of different photoreceptors that may trigger specific biomolecular responses, *e.g.* its ability to sense the direction of light and adapt its flagella beat accordingly (phototaxis).[26,27] In a previous study, we report on our discovery that the flagella-mediated adhesion of *Chlamydomonas* to surfaces can be reversibly switched on and off by light.[28] We showed that the adhesion force of up to several nanonewton in white light is reduced to zero in red light conditions. Although we were able to identify light as a key requirement for the surface colonization, the intermolecular interactions that govern the adhesion of *Chlamydomonas* to surfaces remained elusive.

In this study, we quantify the adhesion forces of *Chlamydomonas reinhardtii* (SAG 11-32b) *in vivo* to a set of ultra-smooth model substrates in controlled environmental conditions. We dissect the fundamental intermolecular interactions underlying microalgal adhesion by tailoring the substrate properties, while the topography of the substrates remains unchanged. We perform single-cell *in vivo* force spectroscopy experiments[29] with the same *Chlamydomonas* cell on different model substrates and provide a statistical comparison of the measured adhesion forces. Thereby, we systematically probe the effect of hydrophobic interactions, van der Waals interactions, and electrostatic interactions on microalgal adhesion.

# 1 Materials and methods

### Substrate preparation and characterization

As substrates, we used non-functionalized as well as functionalized silicon (Si) wafers and magnesium oxide (MgO) substrates. The silicon wafers with native, thin $SiO_2$-layer of approximately 1.7 nm thickness (Si native) and thermally grown, thick $SiO_2$ layer (Si thick) of 150 nm thickness were obtained from Si-Mat (Kaufering, Germany). Magnesium oxide substrates were obtained from Sigma-Aldrich (Germany). In order to obtain hydrophobic substrates, we functionalized silicon wafers (type Si native) with self-assembling silane molecules featuring a $CH_3$ tail group (octadecyltrichlorosilane, OTS, CAS 112-04-9) by following an established recipe.[30]

In the experiments, we used small substrate pieces of approximately 6 mm × 2 mm that were cut from the bulk substrates. These substrate pieces were glued with polydimethylsiloxane (PDMS; Dow Corning, Midland, Michigan, USA; Sylgard® 184 silicon elastomer kit) to a stainless steel substrate holder. After attaching a pair of substrates to the holder, we immersed the substrate holder for three minutes in an ethanol (purity ≥ 99.9%, ROTISOLV® HPLC grade) ultrasonic bath in preparation for experiments. In order to quantitatively compare the adhesion force of the same cell on different substrates, we always attached two different substrates next to each other on the same substrate holder. In experiments featuring substrates cleaned with so-called 'piranha solution', the substrates were cleaned with 'piranha solution' and ethanol, respectively, before attaching them to the holder. The 'piranha solution' contained sulphuric acid ($H_2SO_4$, CAS 7664-93-9, 96.5%) and hydrogen peroxide ($H_2O_2$, CAS 7722-84-1, 30%, stabilised) at a ratio of 1 : 1. The residues of the 'piranha solution' were carefully removed over a period of 90 min by rinsing the substrates with ultra-pure water (Millipore, Milli-Q®, 18.2 MΩ cm, <6 ppb total organic carbon content), the water being replaced at least four times in between.

Table 1 Overview of the surface properties of the substrates employed for cell adhesion force measurements. The cleaning method is provided in parentheses. The uncertainties in the surface energy measurements are estimated from control measurements employing ethylene glycol (CAS 107-21-1) instead of glycerol and the error in the experimentally derived acid–base and Lifshitz–van der Waals components of the probe liquids. The static contact angle of Milli-Q water $\theta_W$ is given to illustrate the surface hydrophobicity resulting from the surface functionalization. The error in the roughness measurement is inferred from independent measurements at different substrate locations and is below 10%

| Substrate | $\gamma^{tot}$/mJ m$^{-2}$ | $\theta_W$/° | rms/nm | pH(*I*) |
|---|---|---|---|---|
| Si native (piranha) | 64(2) | ≤5 | 0.15 | 3[32] |
| Si native (ethanol) | 35(4) | 68(3) | 0.17 | 3[32] |
| Si thick (ethanol) | 37(3) | 66(3) | 0.19 | 3[32] |
| OTS (ethanol) | 23(1) | 113(3) | 0.16 | ≤4[33] |
| MgO (ethanol) | 41(1) | 57(6) | 0.23 | 12.5[34] |

We chose ultra-smooth substrates to dissect the influence of intermolecular interactions on microbial adhesion from the influence of substrate roughness and substrate stiffness. The root-mean-square (rms) surface roughness of the substrates was measured from 1 μm × 1 μm scans using atomic force microscopy (Bruker, Billerica, Massachusetts, USA; DimensionV) in contact mode with a cantilever featuring a nominal tip radius of 7 nm (Olympus Corporation, Tokyo, Japan; OMCL-AC160TS-W2). The Young modulus of the used substrates are on the order of tens of GPa, which is several orders of magnitude stiffer than the extracellular matrix in a biofilm or physiological environments and elastomers.

The surface energy was determined with a three-liquid method[31] using ultra-pure water, Glycerol (CAS 56-81-5) and Bromonapthalene (1-bromonapthalene, CAS 90-11-9) as probe liquids. This method allows to determine the surface energy $\gamma$ from the static contact angles of sessile droplets, which were determined from at least ten independent measurements (dataphysics, OCA).

The isoelectric point pH(*I*), *i.e.* the pH-value at which the substrate carries no mean net charge, is inferred from zeta-potential measurements from literature. The relevant substrate properties are summarized in Table 1.

### Cell cultivation

Wild-type *Chlamydomonas reinhardtii* cells, strain SAG 11-32b, were grown axenically in Tris-acetate-phosphate (TAP) medium (Thermo Fisher Scientific) on a 12 h/12 h day-night cycle in a Memmert IPP 100Plus incubator. The daytime temperature was 24 °C with light intensity of 1 to 2 × 10[20] photons per m$^2$ per s; the nighttime temperature was 22 °C and the light intensity was reduced to zero. Experiments were performed with vegetative cells taken from the cultures in logarithmic growth phase during the daytime on the second to fourth day after incubation.

A small amount of the culture, about 0.1 to 0.2 ml, was injected into the liquid cell to achieve a dilute suspension for force spectroscopy experiments in ambient conditions (24 to 26 °C).

### *In vivo* micropipette force spectroscopy

We studied the adhesion of individual living *Chlamydomonas* cells using micropipette force spectroscopy, following the measurement protocols described in our earlier work[28,29] (see Fig. 1). Micropipette force spectroscopy is an experimental technique that employs the deflection of a force-calibrated micropipette cantilever to measure forces of living cells (see Fig. 1A), inspired by the measurement principle of atomic force microscopy techniques.[29] We determine the deflection of the cantilever using high-resolution optical microscopy combined with an image autocorrelation analysis that features a sub-pixel resolution of the cantilever's deflection. The force sensors were calibrated using the added weight of a variable mass, such as a water droplet attached to a freely suspended micropipette in air, or a reference cantilever. The spring constants of the force sensors employed in this study varied between 0.2 to 1 nN $\mu m^{-1}$, resulting in a force resolution of a few tens of piconewton.

Each individual force–distance cycle consists of a substrate–cell approach, a time delay when the cell is in contact with the substrate, and the retraction of the substrate from the cell (see Fig. 1B). The substrate was moved with a constant speed of 1 $\mu m\ s^{-1}$ and the time delay of 15 s resulted in a total cell-surface contact time of approximately 25 s. This contact time enables the cells to establish the gliding configuration on the substrate,[28] *i.e.* both flagella are spread out at an angle of approximately 180°, representing the natural flagella configuration of *Chlamydomonas* in contact with a substrate. After detachment of the cell from the substrate, the regular flagella beating is recovered after 2 to 15 seconds, as obtained from image sequences of the recovery process recorded at 400 fps. The time between two consecutive force–distance curves was about 60 to 90 seconds to ensure that the regular flagella beating was recovered. The loading rate during a force–distance cycle was 0.2 to 1 nN $s^{-1}$, which is several orders of magnitudes lower than the loading rates in typical bacterial force spectroscopy experiments.[35,36] Within this range of loading rates, the adhesion forces of *Chlamydomonas* were found to be independent of the loading rate.[28]

All experiments were performed in TAP medium as buffer solution at ambient conditions using white-light illumination. We grasped a *Chlamydomonas* cell with the micropipette force sensor in an optically controlled orientation and probed the adhesion of the *Chlamydomonas* flagella to the model substrates (see Fig. 1A). The cell body does not exhibit any adhesiveness.[28] Before and after all experiments, we controlled the viability of the microalgae by monitoring the beating of their flagella or the pulsing vacuole at the cell apex.

### Experimental procedure

To probe the influence of substrate properties on the adhesion force of *Chlamydomonas*, we performed experiments with the exact same cell on a pair of different substrates that were attached next to each other onto the same substrate holder (see Fig. 1C). On each of the two substrates, we carried out two sets of five individual force–distance curves, resulting in a total of ten measurements with the same cell on each substrate. Switching from one substrate to another involves manual repositioning using the micromanipulators, which typically takes between 1 to 5 minutes. The order of the four sets was varied randomly in order to avoid any potential systematic bias in the measured adhesion forces originating from the experimental procedure.

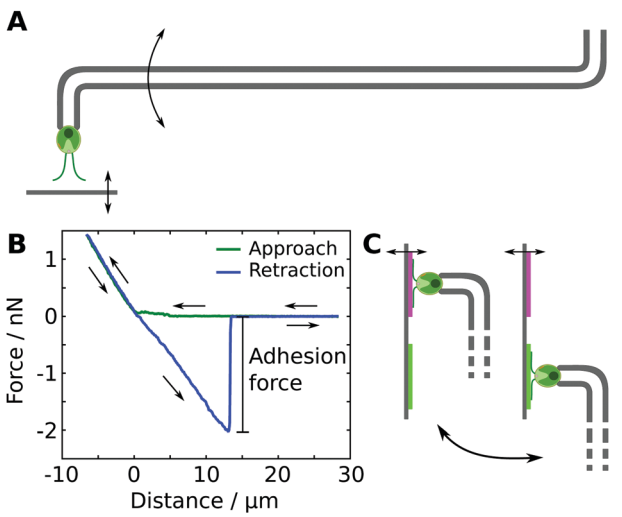


Fig. 1 *In vivo* single-cell adhesion force measurements. (A) Sketch of the measurement principle based on the deflection of a micropipette cantilever (not to scale). (B) Representative force–distance curve extracted from optical measurements of the cantilever deflection. The adhesion force is defined as the maximal force measured during the retraction cycle. The displayed curve represents raw data from a single run without any averaging. (C) The adhesion force of the same cell is probed on two different model substrates. On each substrate, two sets of five force–distance cycles were performed.

## 2 Characterization of the adhesion force distributions

The results of adhesion force measurements of in total 119 *Chlamydomonas* cells are shown in Fig. 2. For each cell, we performed 10 individual force–distance experiments on the Si native reference substrate and calculate the mean adhesion force $\mu$ and the adhesion force spread, characterized by the standard deviation $\sigma$. The mean adhesion forces for different cells vary from almost zero up to 5 nN (see Fig. 2). For each individual cell, the adhesion forces from the 10 individual measurements have a relative standard deviation $\sigma_r = \mu/\sigma$ of a few tens of percent of the mean adhesion value (see inset of Fig. 2).

The mean adhesion forces of 119 cells yields a distribution with mean of 1.77 nN, a median force of 1.48 nN, and a interquartile range of 1.11 nN (25th percentile: 1.10 nN,

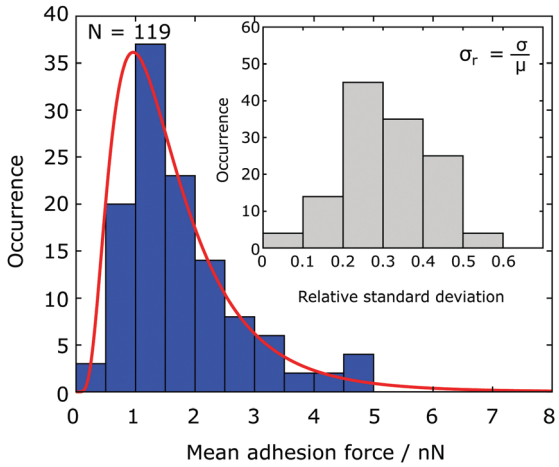


Fig. 2 Statistical distribution of the mean adhesion forces for 119 *Chlamydomonas* cells. The solid red line represents the best fit of a lognormal distribution to the data (see Fig. 6 for a boxplot). Inset: For an individual cell, the relative standard deviation of the adhesion force is a few tens of percent of the mean value.

75th percentile: 2.21 nN, see Fig. 6). The statistical distribution is in excellent agreement with a logarithmic normal distribution,

$$f(x) = \frac{1}{\sqrt{2\pi}\beta x}\exp\left(-\frac{(\ln(x)-\alpha)^2}{2\beta^2}\right),$$

with (dimensionless) fit parameters $\alpha$ = 0.43 and $\beta$ = 0.54, yielding a distribution mean of 1.78 nN and a median of 1.54 nN.

In our experiments, about 6% of all cells exhibited mean adhesion forces larger than approximately 5 nN on the Si native reference substrate. We classify these cells as outliers based on a definition using the interquartile range of the data set (differing by more than 2.5× the interquartile range from the 25th/75th quartile). The data obtained from these cells were excluded from any data analysis (see discussion for further details).

## 3 Force spectroscopy on model substrates with tailored properties

To dissect the intermolecular interactions mediating *Chlamydomonas* adhesion to abiotic substrates, we performed force–distance curves on four different substrate sets, each consisting of a pair of substrates that differ in their surface or subsurface properties. For each set of model substrates, we quantified and compared the adhesion forces using the exact same cells (see Fig. 1C).

### Surface energy

We varied the strength of the short-ranged hydrophobic interactions by performing force spectroscopy experiments on two sets of substrates exhibiting different surface energies. The first substrate set consisted of two pieces of the same silicon wafers that were cleaned in different ways. By cleaning the substrate with a piranha solution, we removed any organic residues from the surface and obtained a hydrophilic substrate (complete wetting, water contact angle $\theta_W \leq 5°$) with a high surface energy. The reference substrate was cleaned with ethanol, which yielded a rather moderate surface energy (see Table 1). The second substrate set contained the reference silicon substrate and a hydrophobic substrate with low surface energy, obtained by functionalizing a silicon wafer with a self-assembled silane monolayer (OTS).

A direct comparison of the adhesion forces recorded on the first substrate set ($N$ = 20 cells) does not show any influence of the substrate cleaning on cell adhesion (Fig. 3A). The characteristic statistical measures of both adhesion force distributions are found to be in excellent agreement (Table 2).

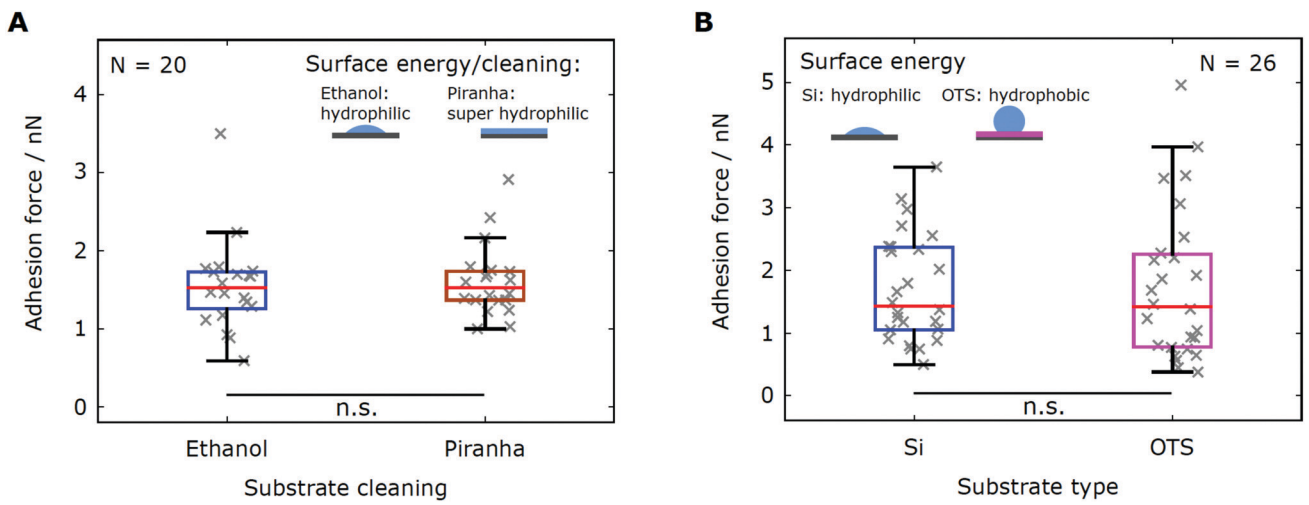


Fig. 3 *Chlamydomonas* adhesion forces on substrates yielding different surface energies. (A) Mean adhesion forces of $N$ = 20 cells on silicon wafers (Si native) that were cleaned with ethanol (blue) and piranha solution (brown), respectively. Results of individual cells are shown in grey. (B) Mean adhesion forces for $N$ = 26 cells on the hydrophilic Si native reference substrate (blue) and a hydrophobized silicon water (OTS, pink). Result of individual cells shown in grey.

 

Table 2 Comparison of the characteristic statistical measures of the adhesion force distributions on all model substrates. The substrate cleaning method is provided in parentheses. The table includes the mean adhesion force $\bar{F}$ as well as the median $F_{0.5}$. The spread of a distribution is characterized by the 25th percentile $F_{0.25}$ and the 75th percentile $F_{0.75}$. The $p$-values are obtained from a Mann–Whitney $U$ test; a $p$-value of $p < 0.05$ is considered significant

| Substrate | Varied substrate properties | Graphs | # of cells | $\bar{F}$/nN | $F_{0.5}$/nN | $F_{0.25}$/nN | $F_{0.75}$/nN | $p$-Value |
|---|---|---|---|---|---|---|---|---|
| Si native (ethanol) | Surface energy | Fig. 3 | 20 | 1.55 | 1.52 | 1.26 | 1.73 | 0.378 |
| Si native (piranha) | | | | 1.61 | 1.52 | 1.36 | 1.74 | |
| Si native (ethanol) | Surface energy | Fig. 3 | 26 | 1.71 | 1.43 | 1.05 | 2.37 | 0.307 |
| OTS (ethanol) | | | | 1.75 | 1.42 | 0.779 | 2.26 | |
| Si native (ethanol) | van der Waals interactions | Fig. 4 | 25 | 1.46 | 1.30 | 1.04 | 1.79 | 0.454 |
| Si thick (ethanol) | | | | 1.50 | 1.50 | 0.919 | 1.75 | |
| Si native (ethanol) | Surface charge | Fig. 5 | 18 | 1.70 | 1.56 | 1.38 | 2.03 | 0.0258 |
| MgO (ethanol) | | | | 1.30 | 1.33 | 0.824 | 1.73 | |

Likewise, force–distance experiments on the second substrate set ($N$ = 26 cells) yield comparable adhesion forces, which is evidenced by the characteristic values of the force distributions (Fig. 3B and Table 2). In summary, the adhesion force distributions obtained from experiments on substrates sets with different surface energies are consistent with each other.

### Van der-Waals interactions

We probe the influence of long-ranged van der Waals (vdW) interactions by comparing silicon wafers with different silicon oxide layer thickness (Si native and Si thick). These model substrates have shown to be well suited to probe the influence of vdW interactions in biological systems, since their surface characteristics are identical within the experimental error while their subsurface contribution is different.[33,37–39] As shown in Fig. 4, adhesion force measurements with the same cells ($N$ = 25 cells) on both types of substrates are in excellent agreement. The adhesion force distributions for *Chlamydomonas* on both types of substrates yield consistent characteristic statistical measures (see Table 2).

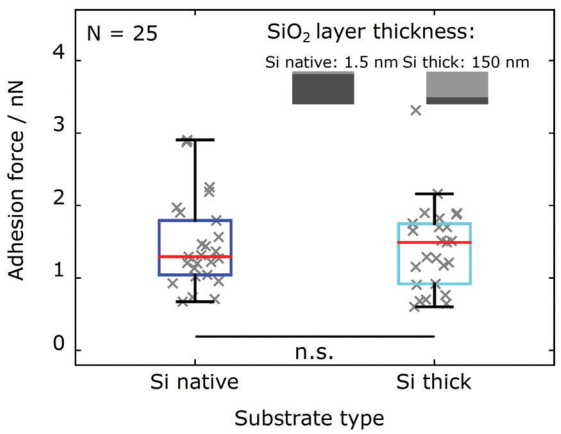


Fig. 4 *Chlamydomonas* adhesion forces on silicon substrates with different silicon dioxide layer thickness. The oxide layer thickness of the substrate alters the contributions from long-ranged van der Waals interactions. Mean adhesion forces of $N$ = 25 cells on Si native (blue) and Si thick (teal) substrates. Results of individual cells shown in grey.

### Electrostatic interactions

In order to determine the effect of electrostatic interactions on the adhesion of *Chlamydomonas* cells to abiotic surfaces, we probe the adhesion forces on substrates exhibiting different surface charges. The reference silicon substrate (Si native) features an isoelectric point pH($I$) $\approx$ 3, see ref. 32, and carries a net negative charge in the TAP buffer solution with a pH $\approx$ 7. In contrast, the magnesium oxide substrate (MgO) has an isoelectric point pH($I$) = 12.5, see ref. 34, resulting in a positive net charge at pH = 7. As all other relevant surface properties of both substrates are comparable (Table 1), we can dissect the influence of surface charges on the adhesion forces of *Chlamydomonas* from any other contributions.

We find that force–distance experiments with the same set of cells ($N$ = 18 cells) yield adhesion forces that are significantly smaller on the MgO substrate as compared to the Si substrate (see Fig. 5 and Table 2). This difference is evidenced by the data sets recorded on MgO being systematically shifted towards smaller adhesion forces as compared to adhesion forces recorded on the Si substrate (see Fig. 5). From the characteristic statistical measures (see Table 2), we estimate that the adhesion forces of *Chlamydomonas* on the MgO substrate were approximately 25% smaller than the adhesion forces on the Si substrate.

In aqueous environment, electrostatic interactions can be tuned by varying the ion concentration in the buffer solution. A higher ion concentration leads to a stronger screening of the electrostatic interactions, *i.e.* smaller Debye length. The standard TAP medium yields a Debye length $1/\kappa \approx 1.8$ nm, which we calculated from the concentration of ions in the medium (obtained from the website of the supplier). In addition to the adhesion experiments in TAP medium, we performed experiments in a nitrogen-deprived minimal medium (NMM) with lower salt concentration (80 μM $MgSO_4$, 100 μM $CaCl_2$, 3.1 mM $K_2HPO_4$, and 3.4 mM $KH_2PO_4$, pH 6.8) yielding a larger Debye length $1/\kappa \approx 2.6$ nm, following the recipe from Berthold *et al.*[40] However, the salt concentration does not only alter the electrostatic interactions, but also directly influences the biology and behavior of *Chlamydomonas*. In the NMM vegetative cells transform into sexually active cells (gametes) that express

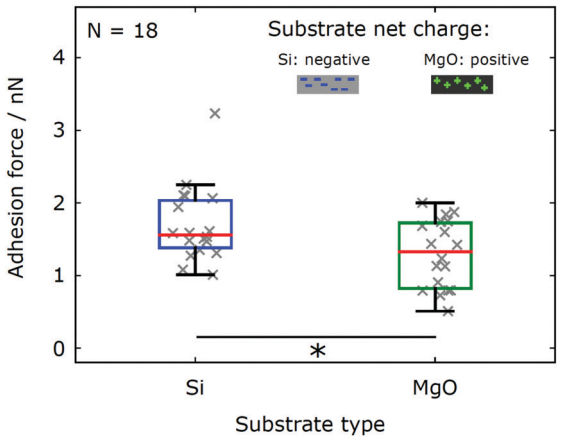


Fig. 5 *Chlamydomonas* adhesion on (negatively charged) Si substrates and (positively charged) MgO substrates. Mean adhesion forces of $N = 18$ cells on the MgO substrate (green) and the Si native reference substrate (blue). Results of individual cells shown in grey.

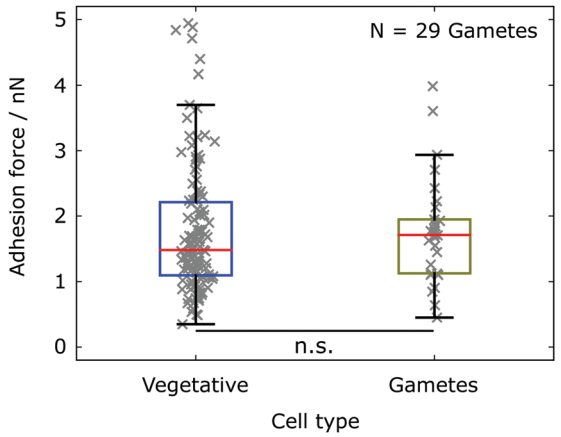


Fig. 6 Mean adhesion forces of *Chlamydomonas* measured in different buffer media yielding different salt compositions and concentrations. The different buffer medium results in a transition from vegetative cells (TAP medium) to gametes (NMM). The adhesion force statistics for gametes (olive, $N = 29$ cells) is compared to the statistics for vegetative cells (blue, see also Fig. 2). The statistical significance test yields $p = 0.2618$.

additional sexual agglutinins on the flagella surface, which are not reported to be involved in the unspecific adhesion to abiotic substrates. We find that *Chlamydomonas* gametes‡ in the NMM exhibit consistent adhesion forces with corresponding vegetative cells in TAP medium (see Fig. 6), despite the different ion concentrations in the two buffer media and the resulting alteration of the Debye length by a factor of 1.5.

# 4 Discussion

### Statistics of adhesion forces

Micropipette force measurements with *Chlamydomonas* cells yielded adhesion forces up to a few nanonewtons. These adhesion forces are comparable to adhesion forces reported for single-cell bacterial adhesion studies.[35,41,42] In these bacterial adhesion studies, a distinct cell-to-cell variability is rather common in force–distance experiments with different cells of the same species. Such adhesion force variations are probably based on spatially inhomogeneous adhesion protein distributions in the bacterial cell wall and heterogeneities in the bacterial population. Ramified signatures in the force–distance curves of bacteria are usually attributed to nanomechanical properties and rupture events of individual adhesive bonds formed by the bacteria's adhesins.[41,43] In contrast to the multitude of different types of adhesins on the bacterial cell wall, adhesion of *Chlamydomonas* to abiotic surfaces is exclusively attributed to one type of adhesion protein, the flagella membrane glycoprotein FMG-1B, which uniformly covers both flagella.[21] A protein-unspecific pronase treatment of the flagella reduced the adhesion force to zero, which confirms that the adhesion of *Chlamydomonas* is mediated by proteins.[28]

On each flagellum there are about 90 000 copies of the adhesion protein FMG-1B, as estimated from polyacrylamide gel electrophoresis.[44] The flagella surface area is about 7.5 $\mu m^2$ (flagella length: 12 μm, diameter: 200 nm), which is conserved for all cells independent of the cell body size. Hence, the average protein density in the flagella membrane would be about 12 000 proteins per $\mu m^2$, based on the estimation by Adair *et al.*[44] The glycosylated ectodomains of these glycoproteins presumably represent the prominent glycocalyx seen in transmission electron micrographs of the flagellum.[45] Although the average number of FMG-1B copies is known for a *Chlamydomonas* population, the amount of flagella membrane proteins of an individual cell depends on the expression of the gene encoding the protein. Protein expression is a stochastic process that leads to variations in the amount of protein in cells, including differences in the protein density in the flagella membrane.[46–49] Thus, we hypothesise that the variations in the measured mean adhesion forces of different cells (see Fig. 2) might be due to a cell-to-cell variability of the FMG-1B density on the flagella.

For a very small subset of cells, we recorded adhesion forces that were up to several times larger than the mean adhesion force of all other cells. The expression of the adhesion-mediating FMG-1B is reported to increase about five-fold upon deflagellation.[50] Such large differences in the protein expression could potentially explain exceptionally high adhesion forces between 5 to 10 nN, assuming that deflagellation and flagella regrowth occurred just before selecting the cell. To avoid any statistical bias from cells that might have experienced flagella regrowth in their history, we exclude the data obtained from these cells.

The relative error of the adhesion force of an individual *Chlamydomonas* cell is in the range of a few tens of percent (see inset of Fig. 2), which might originate from dynamic flagella membrane processes. First, the adhesion-promoting protein FMG-1B is known to redistribute inside the flagellum, as seen by labelling FMG-1B with a fluorescent dye: any labelled FMG-1B is replaced from the flagella within tens of minutes.[51] This phenomenon in the flagella membrane is called 'protein turnover' and could, indeed, result in temporal variations in the

‡ Gametes of both mating types (strain SAG 11-32a and SAG 11-32b) were mixed to observe the sexual mating, as a control for the successful formation of gametes.

protein density during adhesion force measurements from consecutive force–distance curves. Second, the variation of the adhesion force of an individual cell might be affected by the dynamics of adhesive sites. Interference reflection microscopy data of *Chlamydomonas* cells in contact with a substrate suggests that the area of the adhesive contact between flagellum and the substrate is variable.[23] That is, for the same cell, multiple contact sites, which may be different in size, on both flagella may be simultaneously involved in flagella-substrate adhesion. The position of these contact sites changes during gliding, which indicates that these adhesive sites are essential for the mechanical force transduction between flagellum and surface.

### Universal adhesion mechanism

Our experiments revealed that *Chlamydomonas* cells adhere to all tested model substrates with adhesion forces of a few nN. Our results suggest that *Chlamydomonas* features a substrate unspecific and universal mechanism for adhering to abiotic surfaces. A statistical analysis of the adhesion force distributions on complementary model substrates yields three main results: (1) Experiments on substrates with different surface energies display consistent adhesion forces. (2) Substrates that differ in van der Waals interactions do not show any significant differences in the adhesion force distributions. (3) Variation of the electrostatic interactions shows a significant influence on the adhesion forces.

In contrast to our findings for microalgal adhesion, protein-mediated bacterial adhesion to surfaces does usually depend on the physicochemical properties of the substrates.[33,41,42,52,53] For example, single-cell force spectroscopy experiments with *Staphylococcus* yield adhesion forces of several nN on hydrophobic OTS substrates and only tens of pN on hydrophilic Si substrates.[54] These results might be linked to the fact that the adhesins involved in bacterial adhesion are often tailored for attaching to certain biotic substances, *e.g.* the extracellular material in a host or biofilm.[2,3,5,6,41]

The adhesion of *Chlamydomonas* is mediated by the major flagella membrane glycoprotein FMG-1B, which is uniformly distributed on the flagella's surface[55] with an average protein density of about 12 000 proteins per $\mu m^2$ flagella surface (see above). Besides FMG-1B, so far no other protein has been identified to contribute to substrate adhesion, in particular the mastigonemes (flagella appendages of 0.9 to 1.0 μm length and 16 nm diameter) appear not to be involved.[22,56,57] FMG-1B consists of 4149 amino acids (predicted) with an ectodomain of more than 4100 amino acids; the amino acid composition suggests a similar amount of positively and negatively charged amino acids (at pH = 7.4), as well as a similar amount of polar and apolar amino acids. The structure of the protein and its individual domains is unknown, thus, there are no information about hydrophilic or hydrophobic patches, as well as, parts of the protein carrying a significant net charge. Yet, the iodination essay, which identified FMG-1B as the adhesion-mediating protein,[22] qualitatively showed that FMG-1B can bind to polar (glass beads) and apolar (polystyrene microspheres) materials.

The ectodomain of FMG-1B is heavily N-glycosylated,[51] and there is experimental evidence that this glycosylation is (indirectly or directly) responsible for the flagella surface adhesiveness. A treatment with tunicamycin blocks protein glycosylation, which lead to a loss of flagellar adhesiveness, as judged by the ability to bind microspheres, while the flagella length or morphology remained unaffected.[58] A possible indirect influence of protein glycosylation on the adhesive capability is that protein glycosylation leads, among others, to a proper protein folding during the protein synthesis. While the lack of glycosylation does not inhibit protein transport to the surface and protein exposure on the surface of the flagella, the protein stability might be heavily influenced.[59] Consequently, the absence of FMG-1B glycosylation in the flagella membrane would result in a misfolded protein and adhesion-mediating protein domains might not be properly exposed to the substrate. Another possibility is that the tunicamycin treatment resulted in the loss of the carbohydrates and, thus, the protein glycosylation would be directly responsible for the adhesion. The latter functionality of the glycosylation is supported by force spectroscopy studies of the mannose-rich glycosylation of yeast that mediates adhesion forces of individual carbohydrates of tens of piconewton.[60] There is evidence that the carbohydrates of FMG-1B are exposed at the protein surface: anti-protein monoclonal antibodies cannot access the protein epitopes of FMG-1B[51,55] and the glycans normally extend as flexible, hydrated branches by 3 nm and more from the protein surface.[61] The monosaccharide composition of the glycosylation in two *Chlamydomonas* strains was determined,[23] which suggests that the carbohydrates do not carry a net charge, as there are no negatively charged sialic acid residues attached to the carbohydrate.[23,62] Although the general backbone structure of the N-linked glycosylation is known, the structure of the glycosylation in *Chlamydomonas* remains unclear.

In the context of glycoprotein-mediated adhesion, the results of our adhesion force study suggest that the surface-exposed parts of FMG-1B are not predominantly hydrophobic, since otherwise an increased adhesion on the hydrophobized substrates should have been observed. This is supported by the observation that glycan oligosaccharides are predominantly polar[61] and that the protein glycosylation potentially prevents a direct protein/surface interaction so that short-ranged hydrophobic interactions are negligible.

Our results for substrates that carry different net charges suggest that electrostatic interactions play an important role in the adhesion of *Chlamydomonas*, as changing the sign of the substrate's net charge resulted in a systematic shift of the measured adhesion forces. We hypothesise that there might be protein domains (or individual amino acids) carrying opposite charges that both can be exposed to the surface by changing the protein alignment with respect to the surface or conformational changes of the proteins due to electrostatic interactions. Another possibility is that individual side-chains of the protein or individual amino acids undergo an oxidation or, respectively, reduction in contact with a substrate. Such chemical modifications could locally alter the charge of the protein and, thus, influence the electrostatic interactions.

Potential candidates are the amino acids aspargine and glutamine, which can transform to aspartic acid and glutamic acid, respectively. In both forms, these amino acids account for approximately 8% of the total amino acid content in FMG-1B.[23]

## 5 Conclusions

In summary, we find that the protein-mediated adhesion of *Chlamydomonas* microalgae to abiotic surfaces is largely independent of the type of substrate. In conjunction with phototaxis and light-switchable adhesion,[28] the ability to adhere to any kind of surface appears highly beneficial for accomplishing optimal conditions for photosynthesis and might have evolved as an evolutionary advantage for *Chlamydomonas*, which dwells in moist habitats exhibiting heterogeneous surface properties and variable light conditions. We present potential mechanisms underlying unspecific protein-mediated adhesion, for which the N-linked glycosylation of the flagella membrane glycoproteins might play a decisive role. As a result of the ability of microalgae to colonize any substrate in aqueous environments, it might be extraordinarily challenging to develop physicochemical pathways, *e.g.* by applying non-toxic surface coatings, to inhibit microalgal adhesion to surfaces in technological settings.

## Conflicts of interest

There are no conflicts of interest to declare.

## Acknowledgements

The authors thank Maike Lorenz from the Göttingen Algae Culture Collection (SAG) for providing the *Chlamydomonas reinhardtii* strains SAG11-32a and SAG11-32b and for fruitful discussions. Open Access funding provided by the Max Planck Society.

## References

1 L. Hall-Stoodley, J. W. Costerton and P. Stoodley, *Nat. Rev. Microbiol.*, 2004, **2**, 95–108.
2 S. N. Abraham, D. Sun, J. B. Dale and E. H. Beachey, *Nature*, 1988, **336**, 682–684.
3 S. J. Hultgren, S. Abraham, M. Caparon, P. Falk, J. W. Geme and S. Normark, *Cell*, 1993, **73**, 887–901.
4 J. Pizarro-Cerdá and P. Cossart, *Cell*, 2006, **124**, 715–727.
5 C. Beloin, A. Roux and J. M. Ghigo, in *Escherichia coli Biofilms*, ed. T. Romeo, Springer Berlin Heidelberg, Berlin, Heidelberg, 2008, pp. 249–289.
6 T. Proft and E. N. Baker, *Cell. Mol. Life Sci.*, 2008, **66**, 613.
7 R. Bos, H. C. van der Mei and H. J. Busscher, *FEMS Microbiol. Rev.*, 1999, **23**, 179.
8 H. J. Busscher, W. Norde and H. C. van der Mei, *Appl. Environ. Microbiol.*, 2008, **74**, 2559–2564.
9 Y. F. Dufrêne, *Trends Microbiol.*, 2015, **23**, 376–382.
10 M. Tarantola, A. Bae, D. Fuller, E. Bodenschatz, W.-J. Rappel and W. F. Loomis, *PLoS One*, 2014, **9**, e106574.
11 N. Kamprad, H. Witt, M. Schröder, C. Kreis, O. Bäumchen, A. Janshoff and M. Tarantola, *Nanoscale*, 2018, **10**, 22504–22519.
12 K. G. Porter, *Am. Sci.*, 1977, **65**, 159–170.
13 C. B. Field, M. J. Behrenfeld, J. T. Randerson and P. Falkowski, *Science*, 1998, **281**, 237–240.
14 B. Finlay and G. Esteban, *Biodiversity & Conservation*, 1998, **7**, 1163–1186.
15 K. R. Arrigo, *Nature*, 2005, **437**, 349–355.
16 M. P. Schultz, *Biofouling*, 2007, **23**, 331–341.
17 M. P. Schultz, J. A. Bendick, E. R. Holm and W. M. Hertel, *Biofouling*, 2011, **27**, 87–98.
18 J. A. Callow, S. A. Crawford, M. J. Higgins, P. Mulvaney and R. Wetherbee, *Planta*, 2000, **211**, 641–647.
19 T. M. Dugdale, R. Dagastine, A. Chiovitti, P. Mulvaney and R. Wetherbee, *Biophys. J.*, 2005, **89**, 4252–4260.
20 E. H. Harris, *Annu. Rev. Plant Physiol. Plant Mol. Biol.*, 2001, **52**, 363–406.
21 E. H. Harris, D. B. Stern and G. B. Witman, *The Chlamydomonas Sourcebook*, Academic Press, London, 2nd edn, 2009.
22 R. A. Bloodgood and L. J. Workman, *Cell Motil.*, 1984, **4**, 77–87.
23 R. A. Bloodgood, in *Ciliary and Flagellar Membranes*, ed. R. A. Bloodgood, Springer US, Boston, MA, 1990, ch. Gliding Motility and Flagellar Glycoprotein Dynamics in Chlamydomonas, pp. 91–128.
24 J. A. Laib, J. A. Marin, R. A. Bloodgood and W. H. Guilford, *Proc. Natl. Acad. Sci. U. S. A.*, 2009, **106**, 3190–3195.
25 S. M. Shih, B. D. Engel, F. Kocabas, T. Bilyard, A. Gennerich, W. F. Marshall and A. Yildiz, *eLife*, 2013, **2**, e00744.
26 K. W. Foster and R. D. Smyth, *Microbiol. Rev.*, 1980, **44**, 572–630.
27 K. W. Foster, J. Saranak, N. Patel, G. Zarilli, M. Okabe, T. Kline and K. Nakanishi, *Nature*, 1984, **311**, 756–759.
28 C. T. Kreis, M. Le Blay, C. Linne, M. M. Makowski and O. Bäumchen, *Nat. Phys.*, 2018, **14**, 45–49.
29 M. Backholm and O. Bäumchen, *Nat. Protoc.*, 2019, **14**, 594–615.
30 M. Lessel, O. Bäumchen, M. Klos, H. Hähl, R. Fetzer, M. Paulus, R. Seemann and K. Jacobs, *Surf. Interface Anal.*, 2015, **47**, 557–564.
31 C. van Oss, *Colloids Surf., A*, 1993, **78**, 1–49.
32 L. Bousse, S. Mostarshed, B. V. D. Shoot, N. de Rooij, P. Gimmel and W. Göpel, *J. Colloid Interface Sci.*, 1991, **147**, 22–32.
33 P. Loskill, H. Hähl, N. Thewes, C. T. Kreis, M. Bischoff, M. Herrmann and K. Jacobs, *Langmuir*, 2012, **28**, 7242–7248.
34 M. Robinson, J. A. Pask and D. W. Fuerstenau, *J. Am. Ceram. Soc.*, 1964, **47**, 516–520.
35 N. Thewes, A. Thewes, P. Loskill, H. Peisker, M. Bischoff, M. Herrmann, L. Santen and K. Jacobs, *Soft Matter*, 2015, **11**, 8913–8919.
36 N. Thewes, P. Loskill, C. Spengler, S. Hümbert, M. Bischoff and K. Jacobs, *Eur. Phys. J. E: Soft Matter Biol. Phys.*, 2015, **38**, 140.
37 K. Autumn, M. Sitti, Y. A. Liang, A. M. Peattie, W. R. Hansen, S. Sponberg, T. W. Kenny, R. Fearing, J. N. Israelachvili and

 

R. J. Full, *Proc. Natl. Acad. Sci. U. S. A.*, 2002, **99**, 12252–12256.
38 P. Loskill, J. Puthoff, M. Wilkinson, K. Mecke, K. Jacobs and K. Autumn, *J. R. Soc., Interface*, 2012, **10**, 20120587.
39 P. Loskill, H. Hähl, T. Faidt, S. Grandthyll, F. Müller and K. Jacobs, *Adv. Colloid Interface Sci.*, 2012, **179**, 107–113.
40 P. Berthold, S. P. Tsunoda, O. P. Ernst, W. Mages, D. Gradmann and P. Hegemann, *Plant Cell*, 2008, **20**, 1665–1677.
41 R. M. A. Sullan, A. Beaussart, P. Tripathi, S. Derclaye, S. El-Kirat-Chatel, J. K. Li, Y.-J. Schneider, J. Vanderleyden, S. Lebeer and Y. F. Dufrene, *Nanoscale*, 2014, **6**, 1134–1143.
42 G. Zeng, T. Müller and R. L. Meyer, *Langmuir*, 2014, **30**, 4019–4025.
43 R. M. A. Sullan, J. K. Li, P. J. Crowley, L. J. Brady and Y. F. Dufrêne, *ACS Nano*, 2015, **9**, 1448–1460.
44 W. Adair, C. Hwang and U. W. Goodenough, *Cell*, 1983, **33**, 183–193.
45 R. A. Bloodgood and G. S. May, *J. Cell Biol.*, 1982, **93**, 88–96.
46 H. McAdams and A. Arkin, *Proc. Natl. Acad. Sci. U. S. A.*, 1997, **94**, 814–819.
47 M. B. Elowitz, A. J. Levine, E. D. Siggia and P. S. Swain, *Science*, 2002, **297**, 1183–1186.
48 J. R. S. Newman, S. Ghaemmaghami, J. Ihmels, D. K. Breslow, M. Noble, J. L. DeRisi and J. S. Weissman, *Nature*, 2006, **441**, 840–846.
49 A. Sigal, R. Milo, A. Cohen, N. Geva-Zatorsky, Y. Klein, Y. Liron, N. Rosenfeld, T. Danon, N. Perzov and U. Alon, *Nature*, 2006, **444**, 643–646.
50 G. J. Pazour, N. Agrin, J. Leszyk and G. B. Witman, *J. Cell Biol.*, 2005, **170**, 103–113.
51 R. A. Bloodgood, M. P. Woodward and N. L. Salomonsky, *J. Cell Biol.*, 1986, **102**, 1797–1812.
52 R. Yongsunthon and S. K. Lower, *J. Electron Spectrosc. Relat. Phenom.*, 2006, **150**, 228–234.
53 A. Beaussart, S. El-Kirat-Chatel, R. M. A. Sullan, D. Alsteens, P. Herman, S. Derclaye and Y. F. Dufrêne, *Nat. Protoc.*, 2014, **9**, 1049–1055.
54 N. Thewes, P. Loskill, P. Jung, H. Peisker, M. Bischoff, M. Herrmann and K. Jacobs, *Beilstein J. Nanotechnol.*, 2014, **5**, 1501–1512.
55 R. A. Bloodgood, in *The Chlamydomonas Sourcebook*, ed. E. H. Harris, D. B. Stern and G. B. Witman, Academic Press, London, 2nd edn, 2009, pp. 309–368.
56 R. A. Bloodgood, *J. Cell Biol.*, 1977, **75**, 983–989.
57 S. Nakamura, G. Tanaka, T. Maeda, R. Kamiya, T. Matsunaga and O. Nikaido, *J. Cell Sci.*, 1996, **109**, 57–62.
58 R. A. Bloodgood, *Adv. Mol. Cell Biol.*, 1987, **1**, 97–130.
59 H. Lodish, A. Berk, P. Matsudaira, C. A. Kaiser, M. Krieger, M. P. Scott, S. L. Zipursky and J. Darnell, *Molecular Cell Biology*, W. H. Freeman and Company, New York, 2004.
60 D. Alsteens, V. Dupres, K. M. Evoy, L. Wildling, H. J. Gruber and Y. F. Dufrêne, *Nanotechnology*, 2008, **19**, 384005.
61 A. Helenius and M. Aebi, *Annu. Rev. Biochem.*, 2004, **73**, 1019–1049.
62 P. Hermentin, R. Witzel, E.-J. Kanzy, G. Diderrich, D. Hoffmann, H. Metzner, J. Vorlop and H. Haupt, *Glycobiology*, 1996, **6**, 217–230.